Supporting Information

Determination of the Three-dimensional Structure of Ferrihydrite Nanoparticle Aggregates

Benjamin A. Legg, Mengqiang Zhu, Luis R. Comolli, Benjamin Gilbert, Jillian F. Banfield

Autocorrelation Functions:
Figure 1 is an example of the power law fits, which are used to extract fractal dimension, showing all of the autocorrelation functions obtained from a single tomogram, with each curve representing a distinct subvolume. Note, in particular, the high degree of scatter that occurs at large correlation lengths, which necessitates the analysis of multiple tomographic volumes, in order to obtain reliable fractal dimensions.
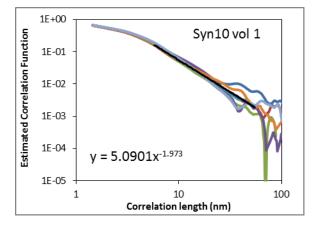

Figure 1: Autocorrelation functions esimtated from Syn10 vol 1, using Equation 7 (main text). Each curve corresponds to a separate subvolume. The best average fit to the fractal region, shown by the black line, has a power law exponent of -1.973, which corresponds to a fractal dimension of 1.03.

Tomograms:

Figure 2 and Figure 3 show two different tomograms obtained for Syn10, and demonstrate how the tomograms are divided into subvolumes for the purposes of processing. These examples demonstrate that not all subvolumes are evenly filled, thus a subvolume such as S15 (from Figure 2 (A) was not used for analysis, but the other volumes were.
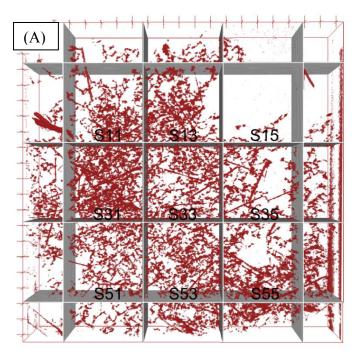

Figure 2: Syn10 vol 2 segmented tomogram, with subvolumes S11 through S55 designated and labeled. During data acquisition, initial pixel size is 0.5423 nm. Each subvolume is a cube, 278 nm edge length. After downsampling for autocorrelation function analysis, each subvolume is a 128x128x128 voxel cube. This sample contained extremely thin ice, and does not completely fill the subvolume in the directions into and out of the page.
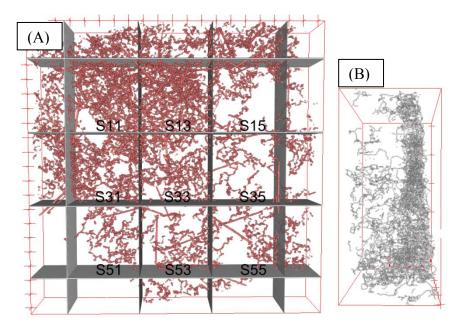
Figure 3: (A) Tomographic reconstruction of Syn10 vol3, showing the subsections that were used for tomographic analysis. (B) Side view of section S11, skeletonized for visual clarity. Note that the ice here is thin, and a thick surface layer of nanoparticles has formed on one of the ice surfaces (right hand size of the image).

Figure 3 , in particular, shows a wide range of structures and particle densities. Sections S11, S13, and S31 all show higher than average particle densities and significant surface reconstruction. These volumes had fractal dimensions (estimated using Equation 7, main text) of 1.9, 1.4, and 1.7, respectively. These values are higher than average for Syn10. However, particle packing density is not the only factor determine fractal dimension, for example, S13 has a higher particle density than S31, but a lower fractal dimension. Close analysis reveals that the distribution of particles within the volume is critical. Examination of volume S11 shows that over half of the particles have accumulated in a dense interfacial layer, as shown in Figure 3 (B). This explains the apparently high (2-dimensional) fractal dimension estimated for that volume, because the dense interfacial layer is, in essence, a two-dimensional object.

Structures with lower particle density do have a tendency toward lower fractal dimension. In fact, S35 and S53 show low fractal dimensions of 1.25 and 0.83, respectively. Close inspection of these volumes shows very similar structures. The very low estimated value for S53 should be regarded as a statistical fluctuation in the local correlation function due to finite sampling size.

3

Calibration Volumes:

In order to "calibrate" the autocorrelation function based approach, computationally generated aggregates were also analyzed. Ten aggregates were generated using the DLA-nd computer program. Five aggregates contained 20,000 particles, five aggregates contained 100,000 particles. The central portion of the aggregate was extracted into a three-dimensional volume for processing. Samples are provided in Figure 4.
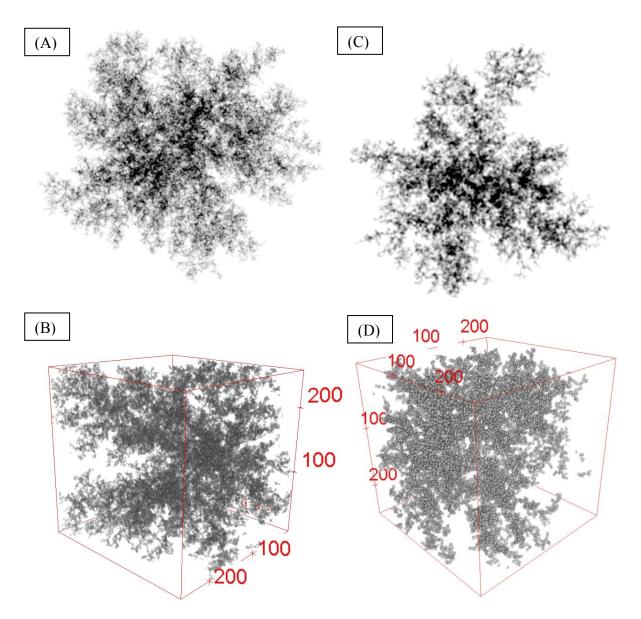

Figure 4: (A) Projection view of a computationally generated DLA based aggregated containing 100,000 particles. (B) 3D volume extracted from the center of this aggregate, for use in calibrating the fractal dimension analysis. Volume is 256x256x256 voxels. (C) Projection view of a computationally generated DLA based aggregated containing just 20,000 particles, the image is scaled by maximum particle extent, so individual particles appear larger. (D) 3D volume extracted from the center of this aggregate.

Notes on SAXS Fitting:

The SAXS structure function determined by Texeira is provided below:

Equation 1

$$S(q) = 1 + (qR_p)^{-d_f} \frac{d_f \Gamma(d_f - 1)}{[1 + (q\xi)^{-2}]^{(d_f - 1)/2}} \sin\left[(d_f - 1) \operatorname{atan}(q\xi)\right]$$

Although apparently complicated, the primary effect of fractal dimension in this function is reflected by the term $(qR_p)^{-d_f}$, which determines the power-law slope of the scattering function at moderate-to-low q-ranges. The additional terms in this function simply determine the high and low q-range behavior.

As we noted in the main text, the full scattering intensity must be determined by multipliting the aggregate structure factor, with the scattering function of the ensemble of primary particles. (This is discussed in greater detail by Texeira). In this study, we assume spherical primary particles. The scattering function for spherical particles is readily available in many texts, and is given in the Texeira paper as follows (we have changed most of the variables for consistency with our paper).

Equation 2

$$f(s) = V^2 \Delta\rho^2 \left(3(qR_p)^{-3}\left[\sin(qR_p) - qR_p \cos(qR)\right]\right)^2$$

The scattering function for the Gaussian distribution of particles is obtained by a weighted average.

Just as the scattering for an ensemble of primary particles with different size can be determined by a weighted average, the scattering for an ensemble of different-sized aggregates can also be obtained. Thus, we obtain the scattering function for a polydisperse ensemble as follows:

Equation 3

$$S_{ensemble}(q) = \frac{\sum N(n)S(q,n)}{\sum N(n)}$$

This basic weighting-approach was utilized by Nicolai *et al*, in their study of polydispersity effects (although it was expressed with a slightly different language). Here, n represents the number of primary particles within an aggregate, while $N(n)$ represents the number of aggregates with that size. The functional form for $N(n)$ can be obtained from Equation 4 of the main text. In order to implement Equation 3, we must determine $S(q,n)$. This can be calculated directly from the Teixeira formula, when it is recognized that a scaling law exists relating the number of particles in a cluster to the cluster cutoff size, $\xi \cong R_p n^{-d_f}$. The ensemble scattering profile then becomes a function of R_p, ΔR_p, d_f, τ, and n_c, which can be easily calculated.